Molecular Desorption by a Moving Contact Line

Sylvain Franiatte, Philippe Tordjeman, and Thierry Ondarçuhu
Institut de Mécanique des Fluides de Toulouse (IMFT), Université de Toulouse, CNRS, 31400 Toulouse, France

(Received 16 March 2021; accepted 8 July 2021; published 5 August 2021)

The interaction of the contact line with topographical or chemical defects at the nanometer scale sets the macroscopic wetting properties of a liquid on a solid substrate. Based on specific atomic force microscopy (AFM) experiments, we demonstrate that molecules physically sorbed on a surface are removed by a dynamic contact line. The mechanism of molecules desorption is directly determined by the capillary force exerted at the contact line on the molecules. We also emphasize the potential of AFM to clearly decorrelate the effects of topographical and chemical defects and monitor, with a subsecond time resolution, the dynamics of molecules adsorption on a surface.

DOI: 10.1103/PhysRevLett.127.065501

It is remarkable that the contact angle of a macroscopic sessile drop depends on the surface properties at the molecular scale [1,2]. Both the topography and the chemical nature of the substrate largely influence its wetting properties [3,4]. For example, nanometric asperities can make a surface superhydrophilic or superhydrophobic [5,6], whereas a molecule monolayer [7,8] or an atomic thick coating [9] modifies the wettability of the underlying substrate. Such surface nanostructuration or functionalization is ubiquitous in natural systems and industrial processes [10,11] but can also result from the detrimental contamination by particles or chemical species [12,13]. The contact line is extremely sensitive to both types of defects at nanometric scale, leading to the poorly understood contact angle hysteresis issue [14–17]. We address here the fundamental question of a possible action of the contact line on the surface at molecular scale. We want to know if molecules adsorbed at the surface can be desorbed by the contact line in motion. This mechanism may be universal since the molecules physisorption energy and the capillary energy are both of the order of a few k_BT, where k_B is the Boltzmann constant and T the temperature. It is known that the capillary force at the contact line can deform a soft solid [18], move particles [19–21], or align DNA [22], but this issue has never been addressed experimentally at the molecular scale.

To answer this question, we use atomic force microscopy (AFM). Dipping nano- or microfibers attached to an AFM cantilever into a liquid while monitoring the capillary force allows measurement of surface energy [23], pinning on individual defects [24,25], and friction at the contact line [26]. Here, we develop specific AFM experiments where a nanoneedle contaminated in air for different time periods is repeatedly dipped into a droplet. We demonstrate that the meniscus which sweeps the needle surface can induce, at the contact line, the local desorption of contaminants and modify the wetting properties of the surface. We also emphasize the potential of AFM to clearly decorrelate the effects of topographical and chemical defects and monitor, with a subsecond time resolution, the dynamics of adsorption of airborne contaminants on a surface.

The experiment is sketched in Fig. 1 and detailed in the Supplemental Material [27]. An AFM tip with a nanoneedle on the end is dipped in and withdrawn from a liquid sessile droplet (4 mm in diameter). This "dipping" cycle is realized at constant velocity V, and the deflection of the cantilever is measured using a Nanowizard 3 JPK AFM. The measured capillary force F is related to the contact angle θ through $F = 2\pi R\gamma\cos\theta$, where R is the radius of the tip and γ the liquid surface tension. Two types of tips are used: a commercial NaugaNeedle tip made in Ag_2Ga alloy [Fig. 1(a)] and homemade tips carved at the end of conventional silicon AFM probes (OLTESPA, Bruker) using a FIB [25] [Fig. 1(b)]. The nanofibers have a radius

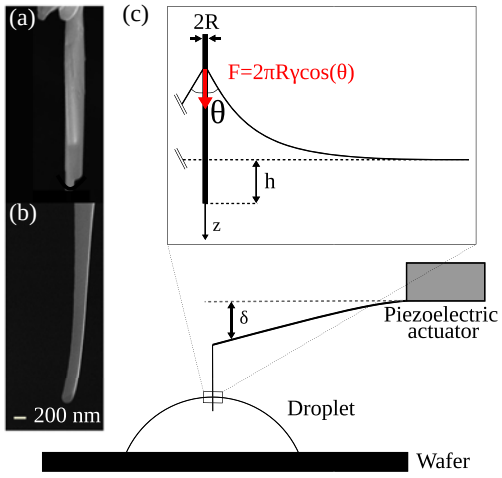

FIG. 1. Scanning electron microscopy images of (a) a NaugaNeedle tip and (b) a silicon tip. (c) Scheme of the setup. Inset: enlargement of the nanomeniscus.

of between 60 and 500 nm, a length of several microns, and the velocity varies from 3 to 200 μm/s. Six liquids of different chemical natures are used to assess the effects of surface tension, viscosity, and volatility: water, ethylene glycol, tetraethylene glycol, glycerol, undecanol, and hexadecane.

To investigate the interaction between a dynamic meniscus and molecules which are physically sorbed at the needle surface, we first performed a series of 100 consecutive dipping cycles at constant V with a needle which was left in ambient air for at least 1 h. The time during which the tip is out of the liquid between two cycles is very short (from typically 15 ms at 200 μm/s to 1 s at 3 μm/s), thereby limiting the contamination by airborne molecules between cycles. The initial force curve measured during the first dipping event with a NaugaNeedle tip in tetraethylene glycol is shown in dark blue in Fig. 2, where the capillary force is plotted as a function of the immersion depth h (see Fig. 1). Once the meniscus is created at $h = 0$, the capillary force fluctuates around a value $F \sim 70$ nN, which corresponds to an advancing contact angle $\theta \sim 60°$. As the tip motion is reversed ($h \sim 3$ μm), the force first increases while the contact line remains pinned by defects, then fluctuates around $F \sim 110$ nN ($\theta \sim 35°$) as the contact line recedes. The meniscus breaks when the contact line reaches the extremity of the tip ($h \sim -2$ μm). The similar fluctuations observed in the advancing and receding branches, with linear parts with the same slope followed by jumps, are a strong indication that the observed contact angle hysteresis is due to the presence of nanometric topographical defects [14,23–25].

The results of 100 consecutive dipping experiments for a NaugaNeedle tip in tetraethylene glycol at $V = 50$ μm/s

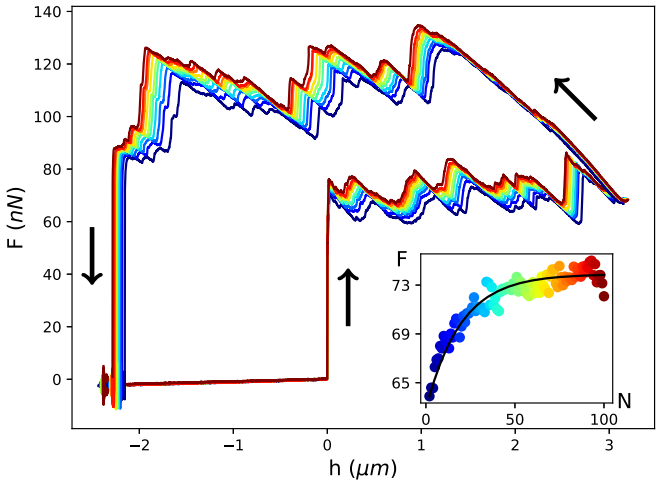

FIG. 2. Overlaid force curves obtained during successive dipping cycles (from dark blue to red) of a NaugaNeedle tip ($R \sim 430$ nm) in tetraethylene glycol at $V = 50$ μm/s. Inset: evolution of the force measured on a topographical defect of the advancing branch as a function of the number of cycles N.

are reported in Fig. 2. The number N of wetting cycles increases as the force curves change from blue to red. Compared to the initial curve, we observe a global enhancement of the capillary force in both the advancing and receding branches when N increases. In the example in Fig. 2, the corresponding contact angles decrease from 60° to 55° for the advancing branch and from 35° to 25° for the receding one. Interestingly, the details of the advancing and receding curves do not show any evolution. Hence, the observed evolution when N increases is due to a change of the tip chemical properties of the needle surface without any modification of its topography. This evolution is followed quantitatively by plotting the force F associated with one peak as a function of N (see an example for the advancing branch in the inset of Fig. 2). The force increases with N from an initial value $F = F_0$ to a stationary constant value $F = F_\infty$. Similar trends are observed for all series performed for different tips and velocities in water, glycerol, glycols, and undecanol. For hexadecane, no measurable evolution is observed: the force curve remains unchanged after a large series of dipping cycles. These results rule out any evaporation or viscosity effects since the saturation vapor pressure varies over 5 decades and the viscosity over 3 dec for the six liquids (see Ref. [27]).

We first want to prove that the change in the wetting properties of the needle surface between the first and the last dipping event of a series is due to the removal of airborne contaminants previously adsorbed on the surface. With that aim, we performed ten successive dipping series similar to the one described above but with a variable waiting time t_p between each series. During t_p, the tip remains out of the liquid and surface contamination by airborne molecules is possible. The results of a typical experiment are reported in Fig. 3, where the characteristic force of one defect is plotted as a function of N for ten successive series of 100 cycles and a waiting time t_p varying from 1 to 30 s. The figure shows that the stationary value F_∞ reached after 100 cycles remains unchanged. Conversely, the initial value F_0 strongly decreases when t_p increases. The relative amplitude $\epsilon = (F_\infty - F_0)/F_\infty$ vs t_p characterizes this effect for both advancing and receding branches (inset of Fig. 3). The variation of ϵ indicates that, when left in contact with air, the needle is contaminated by airborne molecules which are adsorbed with a characteristic time τ of the order of 10 s. These results have been confirmed for all the needles and polar liquids and show a remarkable reversibility. The fact that when left in contact with air a surface becomes more "hydrophobic" has been reported numerous times in the literature. Common sources of such unintentional contamination are short hydrocarbons (propane, butane) in ambient air [13,30,31] and CO_2 at high gas pressure [32]. Both types of volatile organic compounds are known to increase the hydrophobicity of surfaces. In our experimental conditions (atmospheric pressure), it is reasonable to consider that the more likely

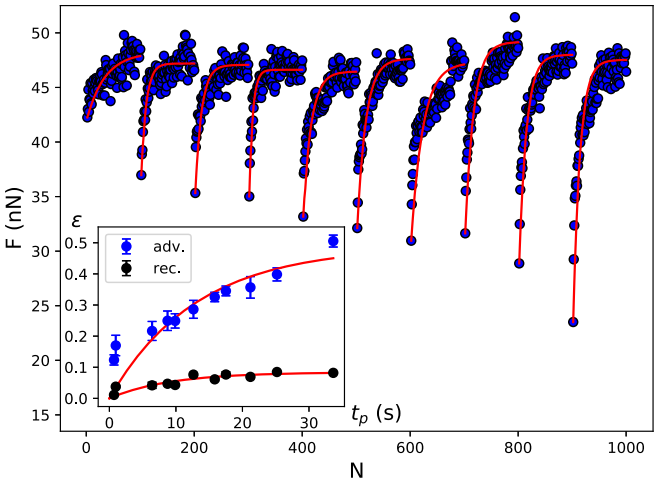

FIG. 3. Evolution of the characteristic force of one peak with the number of wetting cycles for a NaugaNeedle tip ($R \sim 430$ nm) in tetraethylene glycol at $V = 100$ μm/s. The delay time t_p between series is increased from 1 to 30 s. Inset: relative change of the force ϵ as a function of the delay time t_p for the advancing and receding branches. The error bars correspond to a 95% confidence interval.

contaminants are short hydrocarbon chains. This is confirmed indirectly by the fact that hexadecane, which exhibits a chemical nature similar to that of the contaminants, has no effect on the surface properties.

The evolution of the wetting properties observed during one series of dipping events would then be associated with the desorption by the liquid of airborne contaminant molecules adsorbed on the tip surface. We perform specific additional experiments to identify whether desorption is associated with dissolution of molecules in the liquid, helped by the shear stress at the needle wall [33] or with a specific force interaction with the contact line [19,21]. This can be achieved by successive dipping of a predefined part of a needle a large number of times and compare the force curves on the whole tip before and after this particular series. As a first example, a force curve is first recorded [green curve in Fig. 4(a)] by dipping the tip about 2 μm into a polar liquid. A series of 1000 dipping events is then performed by limiting the extension of the tip motion to 1 μm. A full force curve is then immediately recorded [red curve in Fig. 4(a)] to evidence the changes that occurred at the tip surface. This experiment confirms that the modification of the tip surface occurs only on the part which was in contact with the liquid a large number of times. The portion of the tip corresponding to a height greater than 1 μm remains strictly identical, whereas the portion which has been immersed 1000 times in the liquid becomes more "hydrophilic." The enlargement in the inset shows that the transition zone is very well defined and that the very fine details of the curves associated with nanosize defects remains mostly unchanged during the process, again going for a change of chemical properties of the tip. To discriminate whether the desorption of the contaminating molecules

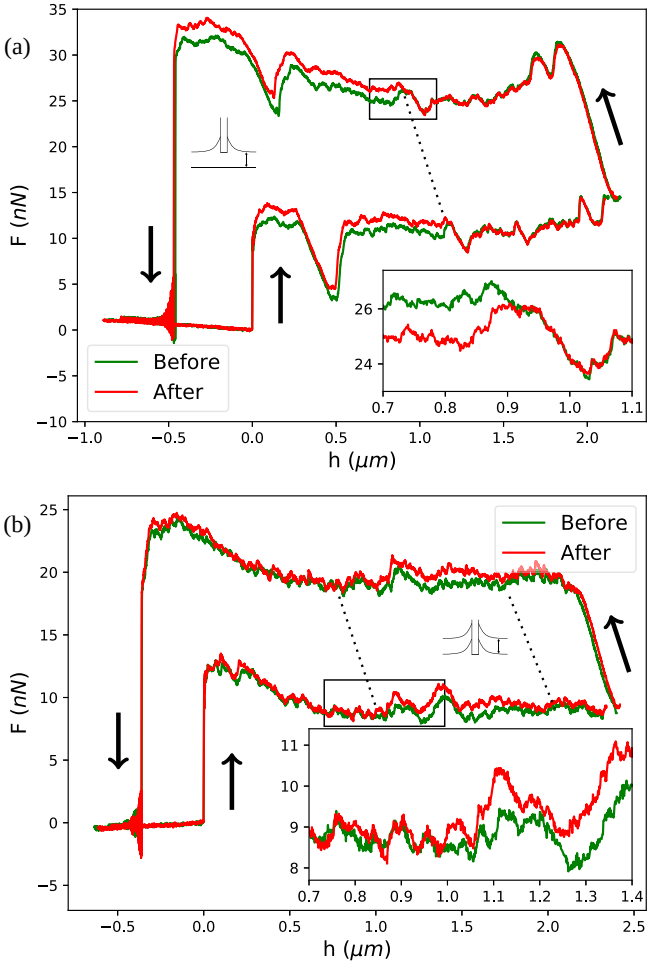

FIG. 4. Force curves before and after 1000 partial dipping for two different homemade tips ($R \sim 60$ nm) and $V = 50$ μm/s with glycerol. (a) Only the extremity of the tip is dipped into the liquid. (b) Only the intermediate zone between $h \sim 1$ μm and $h \sim 2$ μm is swept by the contact line. The dotted line indicates the limits of these zones.

is due to an effect of debonding by shear under the meniscus or by the tension at the contact line, we repeat the same procedure by changing the surface which is dipped a large number of times: we perform 1000 cycles with h varying between 1 and 2 μm. The result is reported in Fig. 4(b) and shows that the only zone with h between ~1 and 2 μm is modified and made more hydrophilic. This zone is the only one which was swept 1000 times by the contact line. The extremity of the fiber, with h between ~0 and 1 μm, remains unchanged, whereas it was in contact with the liquid but not with the contact line. This experiment unambiguously demonstrates the action of the contact line in the desorption of contaminating molecules on the surface.

The $F(N)$ curves associated with the desorption of contaminating molecules (inset of Fig. 2) are fitted using an exponential decay function $F = F_\infty + (F_0 - F_\infty)e^{-N/N^*}$. We extract from this procedure the characteristic number N^* of cycles to reach a stationary force and therefore to

TABLE I. Results table for four liquids. $\epsilon^m_{\max}$ is obtained from experiments and $\epsilon^l_{\max}$ is calculated from the values of θ_0 (AFM measurements) and θ_d (from literature) and $\Phi_{\max} = 0.07$. E_{cap} is calculated from Ref. [14].

	θ_0 (deg)	θ_d (deg)	$\epsilon^m_{\max}(\%)$	$\epsilon^l_{\max}(\%)$	E_{cap}/kT
Water	84 ± 3	110 ± 1	34 ± 22	30 ± 1	7.0 ± 1.0
Glycerol	73 ± 3	97 ± 1	32 ± 10	10 ± 2	7.0 ± 1.0
4gly [a]	56 ± 3	80 ± 1	4.4 ± 2.1	4.8 ± 0.2	7.5 ± 1.0
Undecanol	17 ± 3	36 ± 1	0.5 ± 0.1	1.0 ± 0.2	7.5 ± 1.0

[a]Tetraethylene glycol.

desorb the molecules. The ϵ parameter reflects the relative amplitude of this change. The adsorption mechanism is studied through the $\epsilon(t_p)$ curves (inset of Fig. 3), which are fitted by an exponential function $\epsilon = \epsilon_{\max}(1 - e^{-t_p/\tau})$, where τ and $\epsilon_{\max}$ are the characteristic time and maximum amplitude of the effect, respectively. The same procedure is repeated for several tips, liquids, and velocities. For each experiment, we extract the values of N^*, τ, and $\epsilon_{\max}$. We checked that these values are independent of the peak chosen in the force curves within 6% for N^* and 15% for τ and $\epsilon_{\max}$.

Surprisingly, we did not notice any evolution of N^* with the system studied or the velocity. We found that $N^* = 14 \pm 5$ (see the Supplemental Material [27]). This rules out any temporal process, such as, for example, a diffusive desorption of species in the liquid or by viscous stress at the wall, and is consistent with the picture of a process dominated by the tension at the contact line. Note that, in the case of particle removal, no or a weak influence of the contact line velocity is also observed [19,21]. If we now consider the τ value characterizing the contamination of the needle, we find a constant value $\tau = 7 \pm 4$ s, independent of the tip, liquid, and velocity used. This is not surprising, because, during the waiting time t_p between two series, the tip is simply left in the air.

To model our experimental results, we consider a surface with contact angle θ_0 partially covered by contaminant molecules acting as chemical heterogeneities. We first note that the value of $\epsilon_{\max}$ strongly depends on the nature of the liquid (Table I), from $\epsilon_{\max} \sim 0.5\%$ for undecanol to $\epsilon_{\max} > 30\%$ for glycerol and water. These values are used to estimate the maximum fraction $\Phi_{\max}$ of the surface covered by molecules after long contamination. If we name θ_d the contact angle of the liquid on the chemical defect, a Cassie-Baxter approach [34] leads to $\epsilon_{\max} = \Phi_{\max}[(\cos\theta_0 - \cos\theta_d)/\cos\theta_0]$. Using advancing contact angles measured from the experimental force curves in the stationary state for θ_0 and values of advancing contact angles on paraffin wax (to mimic hydrocarbons) from the literature for θ_d [35–38], we show in Table I that the experimental and calculated values of $\epsilon_{\max}$ agree reasonably for $\Phi_{\max} = 0.07$. Assuming dominant contaminant molecules as short hydrocarbon chains [30] with size $d \sim 0.25$ nm, we estimate the maximum coverage to about one molecule per nm^2 of the surface. This is about the density of single silanol groups which are strong adsorption sites on a silica surface [39].

In a second time, we discuss more in detail the mechanism of molecules desorption. If we consider a short alkane (propane, butane) molecule physically sorbed on the surface, its adsorption energy E_{ads} is of the order of 10 kT [40,41], a value too large to allow desorption by thermal energy. The experiment reported in Fig. 4(b) demonstrates that the desorption process occurs at the contact line and that the viscous stress at the wall does not have any effect. This fact is confirmed by the fact that the capillary number $\text{Ca} = \eta V/\gamma \sim 10^{-4} - 10^{-8}$ is small in our experimental conditions and justifies the important result that the contact line velocity has no effect on the desorption. We estimate the capillary energy by considering that sorbed molecules act as chemical defects spaced by a distance $\xi \sim 1$ nm. Then the local (weak) heterogeneity leads to a capillary energy per molecule $E_{\text{cap}} = \gamma\xi^2[(\cos\theta_d - \cos\theta_0)/2\theta_0]^2 \times \ln(L/\xi)$ [14], where L is the perimeter of the fiber. We report in Table I the values of E_{cap} obtained for the four liquids. We obtain capillary energies ranging from $E_{\text{cap}} \sim 7kT$ and $E_{\text{cap}} \sim 7.5kT$ for water, glycerol, tetraethylene glycol, and undecanol. The capillary energy is of the order of the adsorption energy and may allow the removal of molecules from the surface. It is also consistent with the fact that no influence of the liquid used is observed in the experiments despite the large variety of liquid properties.

In conclusion, our results clearly establish that a contact line is able to desorb molecules physically bonded to a surface. We show that the mechanism of desorption at the molecular scale is linked to the force exerted at the triple line on the molecules. This work is based on a very large number of delicate AFM experiments (more than 30 000 dipping cycles for each tip), which points out the robustness and the excellent reproducibility of the results. The great sensitivity of the force measurements enables to measure minute changes of contaminants surface coverage and sheds light on the dynamics of adsorption and desorption of molecules and their consequences on wetting with a 10 ms time resolution. This can explain the variability often observed when one performs contact angle measurements. Another important advance of our Letter is that the detailed analysis of the force curves during consecutive dipping cycles allows one to decorrelate the effects of topography and chemistry, an issue to understand contact angle hysteresis. This Letter paves the way for a better understanding of contact line dynamics through its coupling with molecular processes at the surface. The active role of the contact line also provides a way for a controlled design of surface properties at nanometer scale. It extends the notion of capillary cleaning usually

considered for solid particles [19,20] and shows that ultraclean surfaces at the molecular scale could be obtained by sweeping a meniscus of polar liquids. Our Letter should stimulate theoretical studies or simulations such as molecular dynamics [42] to understand the capillary desorption effect and its consequences on wetting.

[1] P.-G. De Gennes, Wetting: Statics and dynamics, Rev. Mod. Phys. **57**, 827 (1985).

[2] D. Bonn, J. Eggers, J. Indekeu, J. Meunier, and E. Rolley, Wetting and spreading, Rev. Mod. Phys. **81**, 739 (2009).

[3] D. Quéré, Wetting and roughness, Annu. Rev. Mater. Res. **38**, 71 (2008).

[4] D. Y. Kwok and A. W. Neumann, Contact angle measurement and contact angle interpretation, Adv. Colloid Interface Sci. **81**, 167 (1999).

[5] A. Checco, A. Rahman, and C. T. Black, Robust superhydrophobicity in large-area nanostructured surfaces defined by block-copolymer self assembly, Adv. Mater. **26**, 886 (2014).

[6] J. Yuan, X. Liu, O. Akbulut, J. Hu, S. L. Suib, J. Kong, and F. Stellacci, Superwetting nanowire membranes for selective absorption, Nat. Nanotechnol. **3**, 332 (2008).

[7] P. Silberzan, L. Leger, D. Ausserre, and J. Benattar, Silanation of silica surfaces. a new method of constructing pure or mixed monolayers, Langmuir **7**, 1647 (1991).

[8] S. C. Lim, S. H. Kim, J. H. Lee, M. K. Kim, D. J. Kim, and T. Zyung, Surface-treatment effects on organic thin-film transistors, Synth. Met. **148**, 75 (2005).

[9] T. Ondarçuhu, V. Thomas, M. Nunez, E. Dujardin, A. Rahman, C. T. Black, and A. Checco, Wettability of partially suspended graphene, Sci. Rep. **6**, 24237 (2016).

[10] T. Sun, L. Feng, X. Gao, and L. Jiang, Bioinspired surfaces with special wettability, Acc. Chem. Res. **38**, 644 (2005).

[11] L. Wen, Y. Tian, and L. Jiang, Bioinspired super-wettability from fundamental research to practical applications, Angew. Chem., Int. Ed. Engl. **54**, 3387 (2015).

[12] H. F. Okorn-Schmidt, F. Holsteyns, A. Lippert, D. Mui, M. Kawaguchi, C. Lechner, P. E. Frommhold, T. Nowak, F. Reuter, M. B. Piqué *et al.*, Particle cleaning technologies to meet advanced semiconductor device process requirements, ECS J. Solid State Sci. Technol. **3**, N3069 (2013).

[13] Z. Li, Y. Wang, A. Kozbial, G. Shenoy, F. Zhou, R. McGinley, P. Ireland, B. Morganstein, A. Kunkel, S. P. Surwade *et al.*, Effect of airborne contaminants on the wettability of supported graphene and graphite, Nat. Mater. **12**, 925 (2013).

[14] J. F. Joanny and P. G. de Gennes, A model for contact angle hysteresis, J. Chem. Phys. **81**, 552 (1984).

[15] S. Ramos, E. Charlaix, and A. Benyagoub, Contact angle hysteresis on nano-structured surfaces, Surf. Sci. **540**, 355 (2003).

[16] M. Ramiasa, J. Ralston, R. Fetzer, and R. Sedev, The influence of topography on dynamic wetting, Adv. Colloid Interface Sci. **206**, 275 (2014).

[17] H. Perrin, R. Lhermerout, K. Davitt, E. Rolley, and B. Andreotti, Defects at the Nanoscale Impact Contact Line Motion at All Scales, Phys. Rev. Lett. **116**, 184502 (2016).

[18] A. Pandey, B. Andreotti, S. Karpitschka, G. J. van Zwieten, E. H. van Brummelen, and J. H. Snoeijer, Singular Nature of the Elastocapillary Ridge, Phys. Rev. X **10**, 031067 (2020).

[19] P. Sharma, M. Flury, and J. Zhou, Detachment of colloids from a solid surface by a moving air-water interface, J. Colloid Interface Sci. **326**, 143 (2008).

[20] S. Aramrak, M. Flury, and J. B. Harsh, Detachment of deposited colloids by advancing and receding air-water interfaces, Langmuir **27**, 9985 (2011).

[21] A. Naga, A. Kaltbeitzel, W. S. Wong, L. Hauer, H.-J. Butt, and D. Vollmer, How a water drop removes a particle from a hydrophobic surface, Soft Matter **17**, 1746 (2021).

[22] D. Bensimon, A. J. Simon, V. Croquette, and A. Bensimon, Stretching DNA with a Receding Meniscus: Experiments and Models, Phys. Rev. Lett. **74**, 4754 (1995).

[23] M. M. Yazdanpanah, M. Hosseini, S. Pabba, S. M. Berry, V. V. Dobrokhotov, A. Safir, R. S. Keynton, and R. W. Cohn, Micro-Wilhelmy and related liquid property measurements using constant-diameter nanoneedle-tipped atomic force microscope probes, Langmuir **24**, 13753 (2008).

[24] M. Delmas, M. Monthioux, and T. Ondarçuhu, Contact Angle Hysteresis at the Nanometer Scale, Phys. Rev. Lett. **106**, 136102 (2011).

[25] C. Mortagne, K. Lippera, P. Tordjeman, M. Benzaquen, and T. Ondarçuhu, Dynamics of anchored oscillating nanomenisci, Phys. Rev. Fluids **2**, 102201(R) (2017).

[26] S. Guo, M. Gao, X. Xiong, Y. J. Wang, X. Wang, P. Sheng, and P. Tong, Direct Measurement of Friction of a Fluctuating Contact Line, Phys. Rev. Lett. **111**, 026101 (2013).

[27] See Supplemental Material at http://link.aps.org/supplemental/10.1103/PhysRevLett.127.065501, which includes Refs. [28,29], for an experimental section and additional data for the entire set of liquids.

[28] N. Burnham, X. Chen, C. Hodges, G. Matei, E. Thoreson, C. Roberts, M. Davies, and S. Tendler, Comparison of calibration methods for atomic-force microscopy cantilevers, Nanotechnology **14**, 1 (2003).

[29] J. Dupre de Baubigny, M. Benzaquen, L. Fabié, M. Delmas, J.-P. Aimé, M. Legros, and T. Ondarçuhu, Shape and effective spring constant of liquid interfaces probed at the nanometer scale: Finite size effects, Langmuir **31**, 9790 (2015).

[30] D. B. Millet, N. M. Donahue, S. N. Pandis, A. Polidori, C. O. Stanier, B. J. Turpin, and A. H. Goldstein, Atmospheric volatile organic compound measurements during the pittsburgh air quality study: Results, interpretation, and quantification of primary and secondary contributions, J. Geophys. Res. Atmos. **110**, D07S07 (2005).

[31] A. Kurokawa, K. Odaka, Y. Azuma, T. Fujimoto, and I. Kojima, Diagnosis and cleaning of carbon contamination on SiO_2 thin film, J. Surf. Anal. **15**, 337 (2009).

[32] Y. Belmabkhout, R. Serna-Guerrero, and A. Sayari, Adsorption of CO_2 from dry gases on MCM-41 silica at ambient temperature and high pressure. 1: Pure CO_2 adsorption, Chem. Eng. Sci. **64**, 3721 (2009).

[33] J. Dupré de Baubigny, M. Benzaquen, C. Mortagne, C. Devailly, S. Kosgodagan Acharige, J. Laurent, A. Steinberger, J.-P. Salvetat, J.-P. Aimé, and T. Ondarçuhu, AFM study of hydrodynamics in boundary layers around micro- and nanofibers, Phys. Rev. Fluids **1**, 044104 (2016).

[34] A. Cassie and S. Baxter, Wettability of porous surfaces, Trans. Faraday Soc. **40**, 546 (1944).
[35] H. Kamusewitz, W. Possart, and D. Paul, The relation between Young's equilibrium contact angle and the hysteresis on rough paraffin wax surfaces, Colloids Surf. A **156**, 271 (1999).
[36] B. Jańczuk, T. Białopiotrowicz, and A. Zdziennicka, Some remarks on the components of the liquid surface free energy, J. Colloid Interface Sci. **211**, 96 (1999).
[37] J. Shepard and F. Bartell, Surface roughness as related to hysteresis of contact angles. III. The systems paraffin-ethylene glycol-air, paraffin-methyl cellosolve-air and paraffin-methanol-air, J. Phys. Chem. **57**, 458 (1953).
[38] W. R. Good, A comparison of contact angle interpretations, J. Colloid Interface Sci. **44**, 63 (1973).
[39] J. Nawrocki, Silica surface controversies, strong adsorption sites, their blockage and removal. Part I, Chromatographia, **31**, 177 (1991).
[40] S. Funk, J. Goering, and U. Burghaus, Adsorption kinetics and dynamics of small organic molecules on a silica wafer: Butane, pentane, nonane, thiophene, and methanol adsorption on $SiO_2/Si(1\,1\,1)$, Appl. Surf. Sci. **254**, 5271 (2008).
[41] Y. Zhao, Y. Shen, L. Bai, and S. Ni, Carbon dioxide adsorption on polyacrylamide-impregnated silica gel and breakthrough modeling, Appl. Surf. Sci. **261**, 708 (2012).
[42] D. Seveno, T. D. Blake, and J. De Coninck, Youngs Equation at the Nanoscale, Phys. Rev. Lett. **111**, 096101 (2013).